
DataLight: Offline Data-Driven Traffic Signal Control

Liang Zhang¹ Yutong Zhang² Jianming Deng¹ Chen Li³

Abstract

Reinforcement learning (RL) has emerged as a promising solution for addressing traffic signal control (TSC) challenges. While most RL-based TSC systems typically employ an online approach, facilitating frequent active interaction with the environment, learning such strategies in the real world is impractical due to safety and risk concerns. To tackle these challenges, this study introduces an innovative offline data-driven approach, called *DataLight*. *DataLight* employs effective state representations and reward function by capturing vehicular speed information within the environment. It then segments roads to capture spatial information and further enhances the spatially segmented state representations with sequential modeling. The experimental results demonstrate the effectiveness of *DataLight*, showcasing superior performance compared to both state-of-the-art online and offline TSC methods. Additionally, *DataLight* exhibits robust learning capabilities concerning real-world deployment issues. The code is available at <https://github.com/LiangZhang1996/DataLight>.

1. Introduction

Managing and alleviating traffic congestion remains a significant challenge, underscoring the pivotal role of traffic signal control (TSC) in shaping urban mobility. Traditional TSC methodologies, including FixedTime (Koonce & Rodegerdts, 2008), GreenWave (Török & Kertész, 1996), SCATS (Lowrie, 1990), SCOOT (Hunt et al., 1982), and SOTL (Cools et al., 2013), have seen widespread adoption in recent years. However, their dependence on manually designed traffic signal plans or predefined rules limits their

adaptability and flexibility in handling diverse traffic conditions. In contrast, reinforcement learning (RL)-based methods (Sutton & Barto, 2018) have emerged as promising solutions for adaptive TSC, owing to their capacity to dynamically adapt to evolving scenarios. RL-based models such as FRAP (Zheng et al., 2019a), CoLight (Wei et al., 2019b), AttendLight (Oroojlooy et al., 2020), and Advanced-XLight (Zhang et al., 2022) have garnered popularity in the realm of TSC, attributed to their proficiency in learning and adapting to various traffic conditions through interactions with the environment, utilizing a trial-and-error approach.

Most current RL-based methods typically rely on online approaches, entailing the learning of optimal policies through active interaction with the environment (Zheng et al., 2019a; Wei et al., 2019b; Zhang et al., 2022). While online RL is fundamental for adapting to dynamic scenarios and optimizing policies in real-time, it encounters challenges such as the need for extensive, active environmental interactions, which can be costly, time-consuming, and involve safety risks (Fujimoto et al., 2019; Wu et al., 2019; Kumar et al., 2019; 2020). Additionally, the substantial data requirement for satisfactory performance poses a hurdle in environments where data collection is expensive or challenging. As urban mobility and traffic conditions continually evolve, there is an increasing demand for offline RL-based TSC solutions to offer comprehensive insights and optimize traffic flow in a more anticipatory and strategic manner.

Offline RL-based approaches offer a practical solution by facilitating learning from pre-existing datasets, thus eliminating the necessity for real-time interactions and contributing to a reduction in safety and ethical concerns. The utilization of large-scale historical data proves particularly beneficial in the context of TSC, where acquiring new data can be a challenging endeavor. In the realm of offline RL, advanced methodologies include approaches such as conservative Q-learning (CQL) (Kumar et al., 2020) and Decision Transformers (Chen et al., 2021). These techniques effectively transform existing datasets into potent decision-making tools, leveraging insights from a variety of static experiences. Consequently, offline RL-based approaches hold the potential to streamline the learning process, enhancing the practical applicability in various settings and promoting adaptability to complex real-world challenges. Despite the rapid advancement of offline RL, its applica-

*Equal contribution ¹State Key Laboratory of Herbage Improvement and Grassland Agro-ecosystems, College of Ecology, Lanzhou University, Lanzhou 730000, China ²School of Artificial Intelligence, Beijing University of Posts and Telecommunications ³Graduate School of Informatics, Nagoya University, Chikusa, Nagoya 464-8601, Japan. Correspondence to: Jianming Deng <dengjm@lzu.edu.cn>.

tion in TSC remains notably scarce. Furthermore, offline RL methods consistently grapple with unresolved issues of data distribution shift, adversely affecting model scalability. Therefore, applying offline RL to TSC and deriving satisfactory models from it poses a significant challenge.

Inspired by the above motivations, this study introduces an innovative offline data-driven approach named *DataLight* for TSC, aiming to significantly enhance the efficiency of traffic management systems. Specifically, *DataLight* integrates a network equipped with a self-attention mechanism (Vaswani et al., 2017) to proficiently model spatial states, allowing for a more nuanced understanding of traffic dynamics. Furthermore, *DataLight* excels in capturing the intricate dynamics and spatial distributions of vehicles through the meticulous design of effective state representations and reward function. These distinctive features empower *DataLight* to efficiently glean insights from offline data and provide a robust framework for optimizing TSC. The main contributions are structured as follows:

- **An offline data-driven RL-based model:** Unlike other RL-based TSC methods, *DataLight* is an offline data-driven RL approach that eliminates the need for real-time interaction in TSC systems, enhancing its practical applicability across various environments.
- **Innovative design for state and reward function:** *DataLight* captures vehicle dynamics and spatial positioning by monitoring vehicle speeds and segmenting road spaces, enhancing the representation of traffic states and providing a dynamic control of the overall traffic environment.
- **Outperforming state-of-the-art (SOTA) models:** Extensive experimental results demonstrate that *DataLight* outperforms all online and offline SOTA models, establishing a new benchmark for advanced TSC systems.
- **Strong learning capabilities:** *DataLight* exhibits remarkable abilities in learning effective strategies from minimal amounts of offline data and cyclical offline data easily available in the real world, addressing real-world issues.

2. Related Work

2.1. Traditional TSC Methods

Traditional methods heavily rely on hand-crafted traffic signal plans or rules. FixedTime (Koonce & Rodegerdts, 2008) and GreenWave (Török & Kertész, 1996) control necessitate predetermined cycle lengths, fixed phase sequences, and specific phase splits. Actuated control, such as self-organizing traffic lights (Cools et al., 2013), activates traffic signals based on predefined rules and real-time traffic data. Adaptive control, showcased in TSC systems like SCATS (Lowrie, 1990) and SCOOT (Hunt et al., 1982),

involves formulating a set of traffic plans and selecting the optimal one for the current traffic situation based on data from loop sensors. Optimization-based control methods, such as Max Pressure (Varaiya, 2013), conceptualize TSC as an optimization problem within a specific traffic model, adjusting the traffic signal based on observed traffic data. Recently, certain optimization-based approaches, including Max Pressure and Max-QueueLength (Zhang et al., 2023), have supported multi-intersection TSC, demonstrating superior performance compared to RL methods. Advanced-MaxPressure (Zhang et al., 2022), merging principles from actuated control and optimization-based strategies, has attained a SOTA position in the traditional TSC field, surpassing the performance of the majority of RL methods.

2.2. Online RL-based TSC Methods

Online RL approaches are commonly employed in TSC. Typically, various methods develop network structures to enhance TSC performance. FRAP Zheng et al. (2019a) designs a specific network structure to construct phase features and capture phase competition relations with expert manual design, making it capable of handling unbalanced traffic flows. AttentionLight (Zhang et al., 2023) utilizes attention mechanisms to automatically model phase correlation. CoLight (Wei et al., 2019b) adapts a graph attention network (Velickovic et al., 2017) for intersection cooperation. AttendLight (Oroojlooy et al., 2020) employs the attention mechanism to handle various topologies of intersections.

Furthermore, certain methods emphasize the development of effective state representations or reward function to elevate performance. PressLight (Wei et al., 2019a) undergoes enhancements in LIT (Zheng et al., 2019b) and IntelliLight (Wei et al., 2018) by integrating “pressure” into the state and reward function design. AttentionLight (Zhang et al., 2023) utilizes the queue length as both state representation and reward function, leading to an improvement over FRAP. Advanced-XLight (Zhang et al., 2022) utilizes the effective running vehicle number as a state representation.

Other RL techniques can also contribute to improving TSC performance. DemoLight (Xiong et al., 2019) utilizes imitation learning (Ho & Ermon, 2016) to expedite the learning process. HiLight (Xu et al., 2021) empowers each agent to learn a high-level policy, optimizing the objective locally with hierarchical RL (Kulkarni et al., 2016). MetaLight (Zang et al., 2020) employs Meta-learning (Finn et al., 2017) to adapt quickly and stably to new traffic scenarios.

2.3. Offline RL Algorithms

A central concern in offline RL is the extrapolation error, which is the challenge of accurately assessing actions beyond the training distribution. Batch-constrained deep Q-learning (BCQ) (Fujimoto et al., 2019) constrains the action

space to align closely with on-policy data distributions, aiming to reduce extrapolation errors in fixed batch data scenarios. Behavior regularized actor-critic (Wu et al., 2019) mitigates data distribution issues by regulating the policy to closely mirror the behavioral patterns observed in the dataset. Bootstrapping error accumulation reduction (Kumar et al., 2019) tackles bootstrapping errors by constraining action selection. This approach ensures robust learning from fixed data, overcoming limitations present in Q-learning and actor-critic methods, especially in data-sensitive scenarios. CQL (Kumar et al., 2020) addresses issues of overestimation and distributional shifts by acquiring a conservative Q-function, which improves policy performance through the application of a straightforward Q-value regularizer designed for complex data distributions.

Behavior cloning (BC) offers a direct imitation learning approach, allowing an agent to replicate actions demonstrated by expert. This simplifies the learning process by directly mapping states to actions, avoiding the complexities associated with intricate RL strategies. TD3+BC (Fujimoto & Gu, 2021) introduces minimal modifications by incorporating a BC term in the policy update and implementing state input normalization, specifically addressing value estimation errors. Both Trajectory Transformer (TT) (Janner et al., 2021) and Decision Transformer (DT) (Chen et al., 2021) reinterpret offline RL as a sequence modeling challenge, harnessing the power of the transformer architecture. TT employs beam search to model trajectory distributions across various RL domains, while DT streamlines RL by generating optimal actions through a causally masked Transformer, conditioned on desired returns, past states, and actions. However, limited offline RL algorithms have been considered into TSC.

This study introduces DataLight, an innovative offline data-driven approach meticulously crafted to boost the efficiency of TSC. Through the strategic utilization of effective state representations and reward function, DataLight endeavors to optimize traffic signal operations. This optimization is anticipated to result in improved traffic flow, decreased congestion, and an ultimate enhancement in the overall performance of transportation systems.

3. Preliminary

Traffic signal control. TSC involves a comprehensive understanding of the traffic environment, encompassing elements such as the traffic network, vehicle movements, signal phases, and state representations of traffic. Typically, a traffic network is depicted as a directed graph, with intersections and roads corresponding to nodes and edges, respectively. Roads consist of three lanes, serving as the primary channels for vehicle movement. State representations are lane-based to provide a more accurate description of current states.

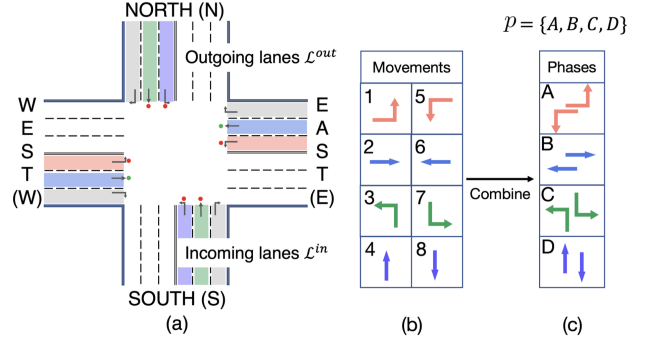


Figure 1. Illustration of intersection structure and traffic signal phases: (a) A standard four-way, three-lane intersection. (b) Eight distinct traffic movements. (c) Four signal phases.

Formally, the set of incoming and outgoing lanes at intersection i can be represented as \mathcal{L}_i^{in} and \mathcal{L}_i^{out} , respectively. Vehicle movements are categorized by their directional paths: left, straight, and right. Each signal phase p is a combination of these traffic movements that are simultaneously permitted. The set of all phases is denoted by \mathcal{P} . For each phase p , \mathcal{L}_p^{in} indicates the involved incoming lanes. As illustrated in Figure 1, in a standard four-way, three-lane intersection, there are typically four signal phases, each with distinct \mathcal{L}_p^{in} . The regulation of vehicle passage, achieved by managing the signal lights for each phase at each intersection, allowed for the effective control of the entire traffic system.

Offline RL. Consider learning within a Markov decision process (MDP) described by the tuple $(\mathcal{S}, \mathcal{A}, P, \mathcal{R}, \gamma)$, where states $s \in \mathcal{S}$, actions $a \in \mathcal{A}$, transition dynamics $P(s|s, a)$, a reward function $r \in \mathcal{R}$, and a discount factor γ . Let s_t , a_t , and r_t represent the state, action, and reward at timestep t . The goal is to formulate a policy that maximizes the expected return $\mathbb{E} \left[\sum_{t=1}^T r_t \right]$ within the MDP. Offline RL involves learning a policy from a pre-determined dataset, which includes single-step transitions $\mathcal{D} = (s_t, a_t, s_{t+1}, r_t)$ without active interaction with the environment. This setup restricts agents from exploring the environment and acquiring additional feedback, introducing complexity to the learning process.

Problem definition. Three distinct TSC methods interacting with the environment result in three offline datasets with distinct quality. These datasets capture the historical trajectories represented as (s_t, a_t, s_{t+1}, r_t) at each timestep t . The RL agent learns an optimal policy to maximize the expected reward across historical trajectories, denoted by

$$\max_{\hat{\pi}} \mathbb{E}_{(s \sim \mathcal{D}, a = \hat{\pi}(s))} [R(s, a)], \quad (1)$$

where $\hat{\pi}(\cdot)$ represents the final learned behavioral policy, denoting the argmax operation in this study. The ultimate goal is to apply the optimally learned policy, derived from offline RL, in scenarios involving multiple intersections. A single agent manages all intersections, ensuring efficient and coordinated traffic control. This approach integrates learning from diverse datasets to optimize signal control in complex, real-world traffic systems.

4. DataLight

4.1. State and Reward Design

State representations. Vehicle speed serves as a crucial indicator of traffic flow dynamics. Specifically, let $V(x)/V_{max}$ denotes the velocity saturation degree, while $1 - V(x)/V_{max}$ indicates the unsaturated degree of each vehicle x . Here, V_{max} represents the maximum permitted velocity. These metrics characterize both static and dynamic states of vehicles. A saturation degree of 1 denotes a vehicle at full speed, while 0 suggests that the vehicle is stopped.

To better capture traffic dynamics, roads near the intersection, extending for 400 meters, are divided into eight 50-meter segments. The vehicle count in each section is monitored, and this segmentation is crucial for model performance, as detailed in Appendix A.1. Additionally, we compute the aggregate of both the velocity saturation and unsaturation degrees across these segments to create comprehensive state representations, including the number of vehicles, the sum of velocity saturation degrees, and the sum of unsaturation degrees under each segmented road section. Note that the total number of vehicles corresponds to the combined sum of the saturation and unsaturation degrees in these segments. Finally, the state representations include the current phase, the number of vehicles, and the total velocity saturation and unsaturation degrees under each road segment. These states provide a detailed and dynamic view of traffic conditions, essential for accurate traffic modeling and the implementation of effective control strategies.

Reward function. Within a 200-meter proximity of the intersection, the reward is calculated as the sum of velocity unsaturation degrees for each approaching lane.

$$r = - \sum_x \left(1 - \frac{V(x)}{V_{max}} \right), \quad (2)$$

where x represents a vehicle within 200-meter range, $V(x)$ denotes its current velocity, and V_{max} is the maximum permitted velocity.

Data from lanes allocated for right turns are excluded from this calculation, recognizing that velocity reductions in these lanes are typically not influenced by the TSC system. The limitation of the assessment range to 200 meters ensures

that vehicle deceleration caused by controls at adjacent intersections does not impact the analysis. A higher reward value indicates a reduction in the number of vehicles affected (either stopped or slowed down) by the intersection signal. This solution effectively captures both the stationary queuing vehicles at intersections and the moving vehicles approaching intersections. It outlines the impact of intersections on traffic flow, considering both stationary and moving vehicles within a strategically determined range.

Action space. Each action corresponds to actuating one phase, allowing vehicles for the respective traffic movements to pass through the intersection. The action space consists of four phases, denoted as $\{A, B, C, D\}$, as illustrated in Figure 1 (c). The RL agent decision-making process involves selecting one of these actions during each fixed action duration at time step t . The RL agent decides to maintain the current phase if $a_t = a_{t-1}$, and switch to another one for the next action duration if $a_t \neq a_{t-1}$.

4.2. Network Structure Design

Spatial encoding (SE). The state inputs undergo an initial embedding layer and are then concatenated based on their spatial correlation, as follows:

$$\mathbf{F}_{l,i} = \text{Emb}(s_{l,i}) \oplus \text{Emb}(s_{l,i+8}) \oplus \text{Emb}(s_{l,i+16}), \quad (3)$$

where i ranges from 0 to 7, corresponding to the 8 segments, and \oplus denotes the concatenate operation. Then, multi-head self-attention (MHA) is employed for SE.

$$\mathbf{F}_l = \text{MHA}(\mathbf{F}_{l,0} \oplus \mathbf{F}_{l,1} \oplus \dots \oplus \mathbf{F}_{l,7}). \quad (4)$$

Feature fusion. The lane features are modeled using MHA based on the phase composition, followed by averaging to obtain the phase feature. The phase feature is then subjected to another MHA operation to capture phase correlations. The resulting correlated phase feature is embedded to derive the Q-values. Additional details of the network design are provided in Appendix A.2.

4.3. Learning Procedure

DataLight undergoes an update process that combines losses of temporal difference (TD), eigensubspace regularization (ER) (He et al., 2023), and CQL (Kumar et al., 2020).

TD loss. The TD loss, also known as the Bellman error, is calculated as follows:

$$\mathcal{L}_{TD}(\theta) = \mathbb{E}_{(s,a,r,s') \sim \mathcal{D}} [y - Q(s, a; \theta)] \quad (5)$$

where θ and $Q(\cdot)$ represent the parameters of the deep Q-learning neural network and its Q-value function, respectively. y denotes the target value, which is calculated by

$$y = r + \gamma \max_{a'} Q(s', a'; \theta^-), \quad (6)$$

where s' and a' denote the next state and action, respectively. γ represents the discount factor, and θ^- is the parameters of the target neural network.

ER loss. At each time step, the ER loss is adjusted towards the 1-eigensubspace, and the regularization term is minimized as follows:

$$\mathcal{L}_{ER}(\theta) = \frac{1}{N} \sum_{n=1}^N \|B_n(\theta) - Z\|_2^2, \quad (7)$$

where $B_n(\cdot)$ represents the Bellman error at the n -th dimension, and $Z = \frac{1}{N} \sum_{n=1}^N B_n(\theta)$. $\|\cdot\|_2^2$ denotes the squared Euclidean norm calculation.

CQL loss. CQL loss is calculated by

$$\mathcal{L}_{CQL}(\theta) = \min_Q \mathbb{E}_{s \sim \mathcal{D}} \left[\log \sum_a \exp(Q(s, a)) - \mathbb{E}_{a \sim \pi(a|s)} [Q(s, a)] \right]. \quad (8)$$

Finally, the total loss of DataLight is formulated as a combination of TD, ER, and CQL losses, with the balance regulated by hyperparameters α and β :

$$\mathcal{L}(\theta) = \mathcal{L}_{TD}(\theta) + \alpha \mathcal{L}_{ER}(\theta) + \beta \mathcal{L}_{CQL}(\theta). \quad (9)$$

5. Experiments

We conducted experiments on CityFlow (Zhang et al., 2019) to answer the following research questions (RQ):

- **RQ1:** How does the performance of DataLight compare with that of SOTA approaches?
- **RQ2:** How do the techniques employed in DataLight, including state and reward design, and SE, impact the learning process?
- **RQ3:** How scalable is DataLight in addressing real-world application issues?

Datasets. Three real-world traffic flow datasets from Ji-Nan (JN), HangZhou (HZ), and New York (NY) were utilized, comprising seven distinct datasets in total (i.e., JN1, JN2, JN3, HZ1, HZ2, NY1, and NY2). We evaluated the performance of DataLight on these datasets, with each dataset offering distinct intersection layouts and traffic flows. JN, HZ, and NY datasets featured a 12-, 16-, and 192-intersection grid. With varying traffic patterns and intersection configurations, these datasets provided a comprehensive test bench to ensure a thorough evaluation of DataLight. The following approaches were employed to generate offline datasets from the JN and HZ datasets:

- **Random offline data (ROD):** A random policy is used to generate a low-quality offline dataset.
- **Medium offline data (MOD):** FRAP is employed to generate a medium-quality offline dataset, reflecting its intermediate performance level.
- **Expert offline data (EOD):** Advanced-CoLight is utilized to produce a high-quality expert-level dataset.
- **Cyclical offline data (COD):** FixedTime is utilized to create an offline dataset with a specific structure, where actions follow a cyclical pattern. This structured data, reflecting real-world scenarios, is utilized to address practical application issues associated with offline methods.

These offline datasets were created using methods that vary in performance, resulting in datasets of different quality. For additional details, refer to Appendix A.3. For the ROD, MOD, and EOD offline datasets, 10 episodes were conducted for each of the five traffic flow datasets, extracting 20K tuples from each (totaling approximately 100K tuples) and discarding excess data. For the COD, one episode generated 11240 transitions at a 20-second action duration.

Furthermore, the offline datasets can be generated at different action durations (refer to Appendix A.3), and DataLight exhibits different performance on these datasets (see Appendix A.4). The performance is evaluated under JN and HZ datasets using an offline dataset with an action duration of 10 seconds, while for NY, 20 seconds are used.

Hyperparameters. The Adam optimizer was utilized with learning rates of $1e-3$ and $2e-4$, respectively. The discount factor γ was set to 0.8. The training process comprises 120 episodes, each undergoing two training epochs. To monitor the training progress, model evaluations were conducted at end of each episode. For a fair comparison, hyperparameters for all offline and online RL baselines were set identical to those of DataLight and AttentionLight, respectively.

Evaluation metric. The average travel time (ATT) (Wei et al., 2019c), a commonly used metric for TSC, is employed to evaluate the performance of DataLight. We performed all experiments three times and calculated the average ATT for the last 10 and 5 episodes across the three repetitions for the online and offline methods, respectively.

5.1. Overall Performance Evaluation Results (RQ1)

We conducted a comparative analysis of DataLight against various baseline models, encompassing traditional approaches (FixedTime, Max Pressure, and Max Queue-Length), online RL-based methods (FRAP, MPLight, PRG-Light, CoLight, AttentionLight, and Advanced-CoLight), and offline RL-based methods (BC, BCQ, and CQL). Note

Table 1. Comparison results with traditional, online RL, and offline RL-based baseline models. A smaller ATT (in seconds) indicates better overall performance evaluation.

Model		JN			HZ		NY		
		JN1	JN2	JN3	HZ1	HZ2	NY1	NY2	
Traditional	FixedTime (Koonce & Rodegerdts, 2008)	429.27	370.34	384.89	497.87	408.31	1507.12	1733.30	
	MaxPressure (Varaiya, 2013)	269.87	239.75	240.03	284.44	327.62	1122.00	1462.96	
	Max-QueueLength (Zhang et al., 2023)	268.87	240.02	238.51	284.32	325.44	1197.59	1551.46	
Online RL-based	FRAP (Zheng et al., 2019a)	299.06	266.19	273.58	321.88	353.89	1192.23	1470.51	
	MPLight (Chen et al., 2020)	297.68	274.32	268.00	313.16	355.35	1321.40	1642.05	
	PRGLight (Chenguang et al., 2021)	291.27	257.52	261.74	301.06	369.98	1283.37	1472.73	
	CoLight (Wei et al., 2019b)	269.47	252.35	249.05	297.64	337.25	1065.64	1367.54	
	AttentionLight (Zhang et al., 2023)	256.36	240.10	237.00	284.85	313.89	1013.78	1401.32	
	Advanced-CoLight (Zhang et al., 2022)	246.42	233.68	229.61	271.62	311.07	970.05	1300.62	
Offline RL-based	BC (Fujimoto & Gu, 2021)	ROD	1488.54	1620.43	1466.24	1635.70	1091.74	2219.42	2354.75
		MOD	439.87	406.43	398.07	522.55	454.22	1273.95	1591.58
		EOD	246.89	225.37	223.81	263.80	319.91	1184.07	1480.33
	BCQ (Fujimoto et al., 2019)	ROD	267.02	237.72	237.24	287.18	338.54	1151.87	1471.87
		MOD	269.50	233.84	237.97	274.84	338.15	1045.30	1362.12
		EOD	253.25	229.51	229.16	267.30	317.99	1061.24	1398.21
	CQL (Kumar et al., 2020)	ROD	275.12	240.87	242.77	285.28	347.48	1195.83	1528.99
		MOD	251.82	234.31	231.73	271.20	326.05	1115.47	1436.03
		EOD	252.37	236.83	234.33	280.84	317.82	1080.97	1421.87
DataLight	ROD	238.68	223.88	221.36	263.24	301.40	1095.40	1367.04	
	MOD	239.13	225.16	222.60	264.75	297.75	920.04	1221.33	
	EOD	234.94	221.31	218.57	261.56	298.18	1075.23	1393.08	

* The values in the gray cells represent the maximum scores among all the different models.

that the offline RL-based methods leverage the state representations and reward function from Advanced-XLight and employ the network structure of AttentionLight. Additionally, both DT (Chen et al., 2021) and TT (Janner et al., 2021) are excluded as offline baselines due to their inability to properly perform the TSC tasks (see Appendix A.5).

Table 1 demonstrates the performance comparison of ATT on real-world datasets. DataLight demonstrates superior performance compared to all traditional and online RL baselines when trained on JN, HZ, and NY datasets. Specifically, on the JN1, JN2, and JN3 datasets, DataLight achieves significant improvements in ATT metric by 4.9%, 5.6%, and 5.1%, surpassing the SOTA Advanced-CoLight. Similarly, DataLight improved by 3.8%, 4.5%, 5.4%, and 6.5% on the HZ1, HZ2, NY1, and NY2 datasets. Furthermore, we trained DataLight on the three distinct offline datasets (ROD, MOD, and EOD) and subsequently evaluated its performance on the JN, HZ, and NY datasets. Even when trained on ROD, DataLight significantly outperformed CQL under EOD, achieving improvements exceeding 5.8% and 5.4% on the JN and HZ datasets, respectively. For the NY1

and NY2 datasets under MOD, DataLight surpassed BCQ by 13.6% and 11.5%, respectively. Overall, DataLight exhibits remarkable potential to surpass SOTA baselines, both in online and offline scenarios, as a pioneering benchmark for addressing challenges in TSC with RL.

5.2. Ablation studies (RQ2)

We conducted separate evaluations of the effects of state representations, reward function, and SE in DataLight, aiming to individually assess their impact and efficacy on the overall performance.

Effects of the designed state representations. The effectiveness of the designed state representations is illustrated in Table 2 and Table B.1. Note that “w/o designed states” denotes that the state representations include only the current phase, the number of vehicles on entering and exiting lanes, queue length on entering and exiting lanes, traffic movement pressure, running vehicles count, and queuing vehicle count. Compared to DataLight without the designed state representations, DataLight with the state representa-

Table 2. The impact of the designed state representations on performance (ATT in seconds) of DataLight.

Model	JN		HZ
	JN1	JN2	HZ1
w/o designed states	244.32	226.82	266.91
DataLight (ROD)	238.68	223.88	263.24
Improvement	↑ 2.31%	↑ 1.30%	↑ 1.37%
w/o designed states	244.12	228.50	269.55
DataLight (MOD)	239.13	225.16	264.75
Improvement	↑ 2.04%	↑ 1.46%	↑ 1.78%
w/o designed states	239.75	224.76	264.03
DataLight (EOD)	234.94	221.31	261.56
Improvement	↑ 2.01%	↑ 1.53%	↑ 0.94%

Table 3. The impact of the designed reward function on performance (ATT in seconds) of DataLight.

Model	JN		HZ
	JN1	JN2	HZ2
w/ pressure	369.63	373.04	355.23
w/ queue length	251.48	230.65	312.07
DataLight (ROD)	238.68	223.88	301.40
Improvement	↑ 5.09%	↑ 2.94%	↑ 3.42%
w/ pressure	269.00	238.42	318.31
w/ queue length	243.48	225.68	305.17
DataLight (MOD)	239.13	225.16	297.75
Improvement	↑ 1.79%	↑ 0.23%	↑ 2.43%
w/ pressure	259.16	230.19	311.20
w/ queue length	238.24	222.70	299.15
DataLight (EOD)	234.94	221.31	298.18
Improvement	↑ 1.39%	↑ 0.62%	↑ 0.32%

tions improved ATT by 2.31%, 1.30%, and 1.37% on the JN1, JN2, and HZ1 datasets when trained on MOD. It also exhibited improvements of 2.04%, 1.46%, and 1.78% on the JN1, JN2, and HZ1 datasets when trained on MOD, and improvements of 2.01%, 1.53%, and 0.94% on EOD. The comparative results indicate the effectiveness of the designed innovative state representations of DataLight, which can significantly enhance the performance of offline data-driven RL strategies.

Effects of the designed reward function. To delve into the performance of DataLight, we scrutinized its correlation with the designed reward function. The effects are showcased in Tables 3 and B.2. Compared to DataLight without the designed reward function, the version with the designed reward function exhibited notable improvements in ATT:

Table 4. The impact of SE on performance (ATT in seconds) of DataLight.

Model	JN		HZ
	JN1	JN2	HZ1
w/o SE	242.15	225.53	264.26
DataLight (ROD)	238.68	223.88	263.24
Improvement	↑ 1.43%	↑ 0.72%	↑ 0.39%
w/o SE	240.02	225.16	264.69
DataLight (MOD)	239.13	225.16	264.75
Improvement	↑ 0.37%	↑ 0.00%	↓ 0.02%
w/o SE	236.51	221.93	262.29
DataLight (EOD)	234.94	221.31	261.56
Improvement	↑ 0.66%	↑ 0.28%	↑ 0.28%

5.09%, 2.94%, and 3.42% on JN1, JN2, and HZ2 when trained on ROD, 1.79%, 0.23%, and 2.43% when trained on MOD, and 1.39%, 0.62%, and 0.32% when trained on EOD. Moreover, particularly when trained on ROD, the designed reward function significantly enhanced DataLight’s performance compared to improvements observed on both MOD and EOD. These results highlight that DataLight with the designed reward function can maintain comparable effectiveness on EOD even when trained on ROD, a crucial factor for achieving a generalized model trained on diverse offline datasets.

Effects of spatial encoding. We also assessed the impact of SE on the performance of DataLight, detailed in Table 4 and Table B.3. In comparison to the model without SE, DataLight with SE showcased improvements in ATT by 1.43%, 0.72%, and 0.39% on JN1, JN2, and HZ1 when trained on ROD, by 0.37% on JN1 when trained on MOD, and by 0.66%, 0.28%, and 0.28% on JN1, JN2, and HZ1 when trained on EOD. Furthermore, with the incorporation of SE, DataLight exhibited superior performance on ROD compared to both MOD and EOD. These results affirm the efficacy of SE in enhancing performance.

5.3. Case studies (RQ3)

Low-data scenario. We evaluated the learning capabilities of DataLight under varying amounts of offline datasets, ranging from 100K, 50K, 30K, 10K, 5K, 1K, to 0.5K. Figure 2 illustrates the impact of data volume on the performance of DataLight. Notably, when the data volume exceeded 30K, the ATT of DataLight trained with the data only showed a slight diminishing effect. However, a noticeable reduction in model effectiveness occurs when the dataset size is less than 10K. Despite this, DataLight maintains satisfactory performance, exhibiting only a minimal

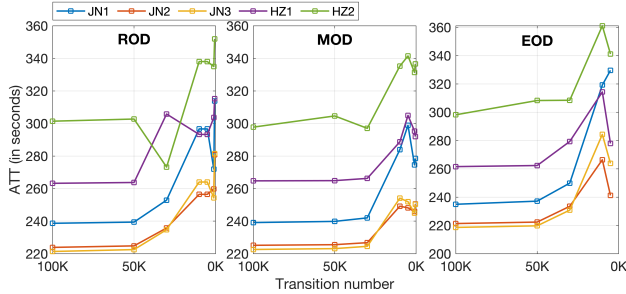


Figure 2. Performance evaluation of DataLight with varying amounts of offline data (ATT in seconds).

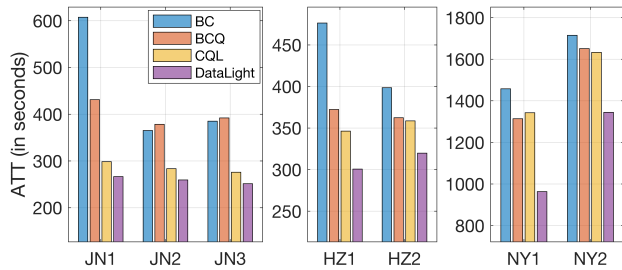


Figure 3. Performance of DataLight on COD (ATT in seconds).

decrease compared to the optimal results. Note that when trained on EOD with less than 5K data, DataLight failed to achieve stable results. This suggests that a larger dataset is more suitable for stabilizing the training on EOD. These findings underscore the reliability of DataLight, showcasing its robust capability to learn well even with limited data.

Learning scenario from COD. In real-world TSC scenarios, FixedTime stands out as the most commonly employed method. To tackle the challenges of real-world learning, we gathered transitions under FixedTime control, each with an action duration of 15 seconds from JN and HZ datasets, creating COD offline data. Figure 3 and Table B.4 illustrate the performance of DataLight when trained on COD. The ATT results of DataLight (depicted in purple) were below 300, 350, and 1400 seconds for the JN, HZ, and NY datasets. Furthermore, DataLight demonstrated a substantial performance advantage over all other offline RL models (BC, BCQ, and CQL), emphasizing its robust learning capabilities from COD. Overall, these results strongly indicate the potential efficacy of deploying and applying DataLight in real-world scenarios.

To thoroughly assess the efficacy of DataLight, we conducted an evaluation that involved the collection and amalgamation of various COD. Subsequently, DataLight was trained on this aggregated dataset and subjected to testing across a range of action durations. The results of this com-

Table 5. Performance evaluation of DataLight under varying action durations when trained with mixed COD (ATT in seconds).

Duration	JN1	HZ1	NY1
10	264.74	266.25	978.94
15	250.19	271.46	959.41
20	253.12	281.09	969.19
25	263.65	292.70	922.30

prehensive evaluation are presented in Table 5 and Table B.5, providing detailed insights into the model’s performance metrics. The outcomes highlight DataLight’s remarkable level of performance, underscoring its robust learning capabilities. Moreover, in specific scenarios, DataLight surpassed the performance of the Advanced-CoLight, further emphasizing its superior performance characteristics.

Additionally, we explored the impact of various action durations on the performance of DataLight. Specifically, we collected and amalgamated various COD. Subsequently, DataLight was trained on this aggregated dataset and subjected to testing across a range of action durations (i.e., 10, 15, 20, and 25 seconds). The results are presented in Table 5 and Table B.5. The outcomes reveal that DataLight achieved a notably high level of performance, thereby underscoring its robust learning capabilities. Furthermore, in certain scenarios, DataLight can match and exceed the performance of the Advanced-CoLight model, thereby reinforcing its superior performance characteristics.

6. Conclusion

This study introduced DataLight, an innovative offline data-driven RL-based approach to TSC. DataLight incorporates effective state representations and a reward function by capturing vehicular speeds and segment road spaces within the TSC environment. The dynamic and spatial representation can enhance traffic conditions through spatial sequential modeling. Experimental results demonstrated that DataLight outperforms SOTA online and offline TSC models. Additionally, DataLight exhibited robust learning capabilities for real-world deployment, evident in two key aspects. First, DataLight achieved satisfactory control results even with limited data. Second, when trained on the easily accessible real-world dataset COD, DataLight significantly outperformed all other offline models.

DataLight has two main limitations. (1) DataLight cannot fully investigate the influence of offline datasets with different action durations on model performance. (2) DataLight lacks the capability to consider the augmentation of neighbor information for policy determination. In future work, we will collect real-world traffic data and develop robust RL

models in practical scenarios, establishing a strong connection between academic research and real-world applications.

Impact Statements

In the context of training models for deployment in real-world scenarios, DataLight holds considerable significance. This importance is attributed to two key factors:

- **Robust Learning Capability:** DataLight demonstrates a robust learning capability, effectively acquiring highly efficient strategies from a wide range of offline data of varying quality, including from limited amounts of COD. The capacity to adapt and learn from varied data sources is crucial for the development of robust and versatile models.
- **Effectiveness with Easily Accessible Real-World Data:** COD represents data that can be easily collected in the real-world. DataLight showcases commendable learning performance with mixed COD datasets. This versatility indicates that DataLight effectively utilizes data that is both abundant and easily obtainable in real-world settings.

These attributes guide us toward a methodology where real-world data can be collected and utilized to train models viable for real-world deployment. DataLight significantly contributes to bridging the gap between academic research and practical applications. It underscores the potential of leveraging real-world data to develop theoretically sound and practically applicable models, enhancing the relevance and impact of academic research in real-world scenarios.

References

Chen, C., Wei, H., Xu, N., Zheng, G., Yang, M., Xiong, Y., Xu, K., and Li, Z. Toward a thousand lights: Decentralized deep reinforcement learning for large-scale traffic signal control. In *Proceedings of the AAAI Conference on Artificial Intelligence*, volume 34, pp. 3414–3421, 2020.

Chen, L., Lu, K., Rajeswaran, A., Lee, K., Grover, A., Laskin, M., Abbeel, P., Srinivas, A., and Mordatch, I. Decision transformer: Reinforcement learning via sequence modeling. *Advances in neural information processing systems*, 34:15084–15097, 2021.

Chenguang, Z., Xiaorong, H., and Gang, W. PRGLight: A novel traffic light control framework with pressure-based-reinforcement learning and graph neural network. In *IJCAI 2021 Reinforcement Learning for Intelligent Transportation Systems (RLAITS) Workshop*, 2021.

Cools, S.-B., Gershenson, C., and D’Hooghe, B. Self-organizing traffic lights: A realistic simulation. In *Advances in applied self-organizing systems*, pp. 45–55. Springer, 2013.

Finn, C., Abbeel, P., and Levine, S. Model-agnostic meta-learning for fast adaptation of deep networks. In *International conference on machine learning*, pp. 1126–1135. PMLR, 2017.

Fujimoto, S. and Gu, S. S. A minimalist approach to offline reinforcement learning. *Advances in neural information processing systems*, 34:20132–20145, 2021.

Fujimoto, S., Meger, D., and Precup, D. Off-policy deep reinforcement learning without exploration. In *International conference on machine learning*, pp. 2052–2062. PMLR, 2019.

He, Q., Zhou, T., Fang, M., and Maghsudi, S. Eigensubspace of temporal-difference dynamics and how it improves value approximation in reinforcement learning. In *Joint European Conference on Machine Learning and Knowledge Discovery in Databases*, pp. 573–589. Springer, 2023.

Ho, J. and Ermon, S. Generative adversarial imitation learning. *Advances in neural information processing systems*, 29, 2016.

Hunt, P., Robertson, D., Bretherton, R., and Royle, M. C. The SCOOT on-line traffic signal optimisation technique. *Traffic Engineering & Control*, 23(4), 1982.

Janner, M., Li, Q., and Levine, S. Offline reinforcement learning as one big sequence modeling problem. *Advances in neural information processing systems*, 34: 1273–1286, 2021.

Koonce, P. and Rodegerdts, L. Traffic signal timing manual. Technical report, United States. Federal Highway Administration, 2008.

Kulkarni, T. D., Narasimhan, K., Saeedi, A., and Tenenbaum, J. Hierarchical deep reinforcement learning: Integrating temporal abstraction and intrinsic motivation. *Advances in neural information processing systems*, 29, 2016.

Kumar, A., Fu, J., Soh, M., Tucker, G., and Levine, S. Stabilizing off-policy Q-learning via bootstrapping error reduction. *Advances in Neural Information Processing Systems*, 32, 2019.

Kumar, A., Zhou, A., Tucker, G., and Levine, S. Conservative Q-learning for offline reinforcement learning. *Advances in Neural Information Processing Systems*, 33: 1179–1191, 2020.

Lowrie, P. SCATS: A traffic responsive method of controlling urban traffic. *Sales information brochure published by Roads & Traffic Authority, Sydney, Australia*, 1990.

- Oroojlooy, A., Nazari, M., Hajinezhad, D., and Silva, J. AttendLight: Universal attention-based reinforcement learning model for traffic signal control. *Advances in Neural Information Processing Systems*, 33:4079–4090, 2020.
- Sutton, R. S. and Barto, A. G. *Reinforcement learning: An introduction*. MIT press, 2018.
- Török, J. and Kertész, J. The green wave model of two-dimensional traffic: Transitions in the flow properties and in the geometry of the traffic jam. *Physica A: Statistical Mechanics and its Applications*, 231(4):515–533, 1996.
- Varaiya, P. Max pressure control of a network of signalized intersections. *Transportation Research Part C: Emerging Technologies*, 36:177–195, 11 2013. doi: 10.1016/j.trc.2013.08.014.
- Vaswani, A., Shazeer, N., Parmar, N., Uszkoreit, J., Jones, L., Gomez, A. N., Kaiser, Ł., and Polosukhin, I. Attention is all you need. *Advances in neural information processing systems*, 30, 2017.
- Velickovic, P., Cucurull, G., Casanova, A., Romero, A., Lio, P., and Bengio, Y. Graph attention networks. *stat*, 1050: 20, 2017.
- Wang, Z., Schaul, T., Hessel, M., Hasselt, H., Lanctot, M., and Freitas, N. Dueling network architectures for deep reinforcement learning. In *International conference on machine learning*, pp. 1995–2003. PMLR, 2016.
- Wei, H., Zheng, G., Yao, H., and Li, Z. IntelliLight: A reinforcement learning approach for intelligent traffic light control. In *Proceedings of the 24th ACM SIGKDD International Conference on Knowledge Discovery & Data Mining*, pp. 2496–2505, 2018.
- Wei, H., Chen, C., Zheng, G., Wu, K., Gayah, V., Xu, K., and Li, Z. PressLight: Learning max pressure control to coordinate traffic signals in arterial network. In *Proceedings of the 25th ACM SIGKDD International Conference on Knowledge Discovery & Data Mining*, pp. 1290–1298, 2019a.
- Wei, H., Xu, N., Zhang, H., Zheng, G., Zang, X., Chen, C., Zhang, W., Zhu, Y., Xu, K., and Li, Z. CoLight: Learning network-level cooperation for traffic signal control. In *Proceedings of the 28th ACM International Conference on Information and Knowledge Management*, pp. 1913–1922, 2019b.
- Wei, H., Zheng, G., Gayah, V., and Li, Z. A survey on traffic signal control methods. *arXiv preprint arXiv:1904.08117*, 2019c.
- Wu, Y., Tucker, G., and Nachum, O. Behavior regularized offline reinforcement learning. *arXiv preprint arXiv:1911.11361*, 2019.
- Xiong, Y., Zheng, G., Xu, K., and Li, Z. Learning traffic signal control from demonstrations. In *Proceedings of the 28th ACM International Conference on Information and Knowledge Management*, pp. 2289–2292, 2019.
- Xu, B., Wang, Y., Wang, Z., Jia, H., and Lu, Z. Hierarchically and cooperatively learning traffic signal control. In *Proceedings of the AAAI Conference on Artificial Intelligence*, volume 35, pp. 669–677, 2021.
- Zang, X., Yao, H., Zheng, G., Xu, N., Xu, K., and Li, Z. MetaLight: Value-based meta-reinforcement learning for traffic signal control. In *Proceedings of the AAAI Conference on Artificial Intelligence*, volume 34, pp. 1153–1160, 2020.
- Zhang, H., Feng, S., Liu, C., Ding, Y., Zhu, Y., Zhou, Z., Zhang, W., Yu, Y., Jin, H., and Li, Z. CityFlow: A multi-agent reinforcement learning environment for large scale city traffic scenario. In *The World Wide Web Conference*, pp. 3620–3624, 2019.
- Zhang, L., Wu, Q., Shen, J., Lü, L., Du, B., and Wu, J. Expression might be enough: Representing pressure and demand for reinforcement learning based traffic signal control. In *Proceedings of the 39th International Conference on Machine Learning*, volume 162 of *Proceedings of Machine Learning Research*, pp. 26645–26654. PMLR, 17–23 Jul 2022.
- Zhang, L., Xie, S., and Deng, J. Leveraging queue length and attention mechanisms for enhanced traffic signal control optimization. In *Joint European Conference on Machine Learning and Knowledge Discovery in Databases*, pp. 141–156. Springer, 2023.
- Zheng, G., Xiong, Y., Zang, X., Feng, J., Wei, H., Zhang, H., Li, Y., Xu, K., and Li, Z. Learning phase competition for traffic signal control. In *Proceedings of the 28th ACM International Conference on Information and Knowledge Management*, pp. 1963–1972, 2019a.
- Zheng, G., Zang, X., Xu, N., Wei, H., Yu, Z., Gayah, V., Xu, K., and Li, Z. Diagnosing reinforcement learning for traffic signal control. *arXiv preprint arXiv:1905.04716*, 2019b.

Supplementary Materials

DataLight: Offline Data-Driven Traffic Signal Control

A. Model study

A.1. Effects of different segments

DataLight’s performance is assessed using different state representations based on different road segmentations. For all offline datasets, actions are set with a duration of 10 seconds. The approach involves segmenting a 400-meter area approaching the intersection into either four or eight segments. The results, as depicted in Table A.1, highlight DataLight’s performance with these diverse state representations. It is observed that DataLight achieves its best performance with the eight segmented states in the JN and HZ datasets. In the NY dataset, the performance differences are minimal. Based on these findings, the eight-segmented state representation is chosen as the default for DataLight.

Table A.1. DataLight performance with different state representations that use four or eight segments (ATT in seconds).

Segments	Dataset	JN			HZ		NY	
		JN1	JN2	JN3	HZ1	HZ2	NY1	NY2
4	ROD	239.98	225.61	222.86	264.51	293.08	1241.08	1571.27
	MOD	240.71	227.48	224.67	266.49	301.21	1212.93	1569.76
	EOD	236.49	223.44	220.47	263.28	298.47	1161.25	1443.57
8	ROD	238.68	223.88	221.36	263.24	301.40	1260.10	1583.87
	MOD	239.13	225.16	222.60	264.75	297.75	1170.28	1464.51
	EOD	234.94	221.31	218.57	261.56	298.18	1214.29	1354.92

A.2. DataLight Network Details

The detailed network of DataLight is described as follows, which consists of four modules:

- **Spatial encoding.** The state inputs undergo an initial embedding layer and are then concatenated based on their spatial correlation, as follows:

$$\mathbf{F}_{l,i} = \text{Emb}(s_{l,i}) \oplus \text{Emb}(s_{l,i+8}) \oplus \text{Emb}(s_{l,i+16}), \quad (\text{A.1})$$

where i ranges from 0 to 7, corresponding to the 8 segments, and \oplus denotes the concatenate operation. Then, multi-head self-attention (MHA) (Vaswani et al., 2017) is employed for SE.

$$\mathbf{F}_l = \text{MHA}(\mathbf{F}_{l,0} \oplus \mathbf{F}_{l,1} \oplus \dots \oplus \mathbf{F}_{l,7}), \quad (\text{A.2})$$

where positional encoding is utilized for SE.

- **Feature fusion.** Multi-head self-attention (MHA) is employed to integrate features from all incoming lanes relevant to each phase:

$$\mathbf{F}^p = \text{Mean}(\text{MHA}(\mathbf{F}_l \oplus \mathbf{F}_k), l, k \in \mathcal{L}_p), \quad (\text{A.3})$$

where p denotes each phase, \mathcal{L}_p is the set of participating entering lanes of phase p .

- **Phase correlation.** The Fused phase feature is processed using MHA to capture inter-phase correlations:

$$\mathbf{F}^{\mathcal{P}} = \text{MHA}(\mathbf{F}^A \oplus \mathbf{F}^B \oplus \mathbf{F}^C \oplus \mathbf{F}^D), \mathcal{P} = \{A, B, C, D\}, \quad (\text{A.4})$$

- **Q-value prediction.** The phase features are further processed to obtain the Q-value of each action:

$$\tilde{q}_d = \text{DuelingBlock}(\text{Embed}(\mathbf{F}^{\mathcal{P}})). \quad (\text{A.5})$$

where DuelingBlock is the dueling module (Wang et al., 2016).

A.3. Details of offline datasets generation

Offline datasets can be generated with different action durations, Table A.2 describes the specific performance of the methods which are used for generating the offline dataset. Apart from COD, each dataset contains 100K transitions. For the COD generated with the action duration as 10s, there is a total of 24480 ($360 \times 12 \times 3 + 360 \times 16 \times 2$) transitions; for the COD generated with the action duration as 15s, there is a total of 16320 ($240 \times 12 \times 3 + 240 \times 16 \times 2$) transitions; while for the COD generated with the action duration as 20s, there is a total of 12240 ($180 \times 12 \times 3 + 180 \times 16 \times 2$) transitions.

Table A.2. Specific methods performance used for generating the offline dataset (ATT in seconds).

Dataset	Action Duraiton	JN			HZ	
		JN1	JN2	JN3	HZ1	HZ2
ROD	10s	590.92	537.05	539.29	577.24	483.43
	15s	559.76	507.28	515.84	555.41	464.70
	20s	560.02	514.37	519.54	572.95	471.69
MOD	10s	321.36	297.76	284.39	308.15	381.81
	15s	289.06	262.40	259.93	308.16	345.31
	20s	282.29	269.97	268.85	313.74	341.57
EOD	10s	247.20	226.13	223.62	264.25	325.94
	15s	246.76	233.85	230.41	271.68	310.25
	20s	254.39	244.20	239.19	282.08	315.91
COD	10s	612.36	549.21	542.83	554.73	462.62
	15s	429.27	370.34	384.89	497.87	408.31
	20s	443.08	369.91	390.17	483.38	404.49

A.4. Model performance with different offline datasets

DataLight is evaluated when trained with different offline datasets. Table A.3 demonstrates the model performance with ATT in seconds. When trained with ROD, MOD, and EOD, DataLight performs best under JN and HZ with the action duration as 10s (which is used to generate the offline datasets). When trained with COD, DataLight performs best among all the dataset with the action duration as 20s. When tested under NY, DataLight consistently performs best with the action duration as 20s.

Table A.3. DataLight performance under different offline datasets (ATT in seconds).

Dataset	Action Duraiton	JN			HZ		NY	
		JN1	JN2	JN3	HZ1	HZ2	NY1	NY2
ROD	10s	238.68	223.88	221.36	263.24	301.40	1260.10	1583.87
	15s	244.43	231.72	227.91	270.56	295.92	1194.52	1513.24
	20s	250.33	243.16	236.95	281.64	308.50	1095.40	1367.04
MOD	10s	239.13	225.16	222.60	264.75	297.75	1170.28	1464.51
	15s	242.51	231.51	227.49	271.00	290.75	1118.07	1467.25
	20s	250.69	243.06	236.15	284.23	297.29	920.04	1221.33
EOD	10s	234.94	221.31	218.57	261.56	298.18	1214.29	1354.92
	15s	241.01	229.68	225.80	268.67	299.68	1216.64	1527.65
	20s	249.01	240.34	234.67	278.76	302.59	1075.23	1393.08
COD	10s	324.98	244.20	273.76	294.08	332.12	1040.38	1427.68
	15s	271.09	252.89	248.89	296.17	326.92	1010.09	1359.39
	20s	266.68	259.53	251.35	300.67	319.80	963.13	1344.77

A.5. Analysis of Decision Transformer

We realize Decision Transformer (DT) (Chen et al., 2021) for TSC according to the original article. All the offline datasets are generated with action duration as 10s. Table A.4 demonstrates the model performance of DT with different configurations. K indicates the sequence length when modeling DT. The returns-to-go is set as -351 according to the gather the trajectory. DT performs better under K=1 than K=2, indicating that the sequential modeling cannot advance the model performance. Furthermore, DT performs better when removing the transformer, indicating modeling returns-to-go, states and action with transformer cannot work. Overall, we conclude that DT cannot be applied for TSC. And the possible reasons include: 1) the special environment of TSC which the long action duration makes the sequential modeling captures the temporal relations hard; 2) the offline datasets are mixed with trajectories from multiple agents, which may make DT agents confused.

Table A.4. The performance of DT under different configurations (ATT in seconds).

Configure	Dataset	JN			HZ	
		JN1	JN2	JN3	HZ1	HZ2
K=1	ROD	779.63	809.38	722.30	514.93	640.53
	MOD	851.77	828.99	796.33	628.81	792.93
	EOD	1295.69	1387.51	1277.11	1173.84	825.32
K=2	ROD	997.04	1004.47	948.26	833.25	630.32
	MOD	1278.78	1366.18	1258.05	1297.03	893.14
	EOD	1225.71	1304.54	1189.28	1185.02	808.74
w/o transformer	ROD	621.98	663.42	617.96	610.07	491.94
	MOD	679.45	626.30	620.78	604.61	501.80
	EOD	898.23	955.31	866.42	873.97	626.35

B. Details of Experimental Results

Table B.1. DataLight performance with and without our proposed state representations (ATT in seconds).

Method	JN			HZ	
	JN1	JN2	JN3	HZ1	HZ2
w/o our states	244.32	226.82	224.42	266.91	303.18
DataLight(ROD)	238.68	223.88	221.36	263.24	301.40
Improvement	↑ 2.31%	↑ 1.30%	↑ 1.36%	↑ 1.37%	↑ 0.59%
w/o our states	244.12	228.50	226.49	269.55	312.88
DataLight(MOD)	239.13	225.16	222.60	264.75	297.75
Improvement	↑ 2.04%	↑ 1.46%	↑ 1.72%	↑ 1.78%	↑ 4.84%
w/o our states	239.75	224.76	222.44	264.03	300.33
DataLight(EOD)	234.94	221.31	218.57	261.56	298.18
Improvement	↑ 2.01%	↑ 1.53%	↑ 1.74%	↑ 0.94%	↑ 0.72%

Table B.2. DataLight performance with and without our proposed reward function (ATT in seconds).

Method	JN			HZ	
	JN1	JN2	JN3	HZ1	HZ2
pressure	369.63	373.04	359.65	312.66	355.23
queue length	251.48	230.65	230.46	268.91	312.07
DataLight(ROD)	238.68	223.88	221.36	263.24	301.40
Improvement	↑ 5.09%	↑ 2.94%	↑ 3.95%	↑ 2.11%	↑ 3.42%
pressure	269.00	238.42	236.78	278.23	318.31
queue length	243.48	225.68	224.45	264.60	305.17
DataLight(MOD)	239.13	225.16	222.60	264.75	297.75
Improvement	↑ 1.79%	↑ 0.23%	↑ 0.82%	↓ 0.06%	↑ 2.43%
pressure	259.16	230.19	231.89	267.77	311.20
queue length	238.24	222.70	220.07	262.36	299.15
DataLight(EOD)	234.94	221.31	218.57	261.56	298.18
Improvement	↑ 1.39%	↑ 0.62%	↑ 0.68%	↑ 0.30%	↑ 0.32%

Table B.3. DataLight performance with and without spatial sequential encoding (ATT in seconds).

Method	JN			HZ	
	JN1	JN2	JN3	HZ1	HZ2
w/o SE	242.15	225.53	224.45	264.26	296.99
DataLight(ROD)	238.68	223.88	221.36	263.24	301.40
Improvement	↑ 1.43%	↑ 0.72%	↑ 1.38%	↑ 0.39%	↓ 1.46%
w/o SE	240.02	225.16	223.43	264.69	303.55
DataLight(MOD)	239.13	225.16	222.60	264.75	297.75
Improvement	↑ 0.37%	↑ 0.00%	↑ 0.37%	↓ 0.02%	↑ 1.91%
w/o SE	236.51	221.93	219.55	262.29	301.83
DataLight(EOD)	234.94	221.31	218.57	261.56	298.18
Improvement	↑ 0.66%	↑ 0.28%	↑ 0.45%	↑ 0.28%	↑ 1.21%

Table B.4. Performance comparison under cyclical offline dataset(ATT in seconds).

Method	JN			HZ		NY	
	JN1	JN2	JN3	HZ1	HZ2	NY1	NY2
BC	607.36	365.27	385.22	476.28	398.54	1457.91	1715.38
BCQ	431.22	378.34	392.17	372.35	362.48	1313.79	1651.10
CQL	431.22	378.34	392.17	372.35	362.48	1313.79	1651.10
DataLight	266.68	259.53	251.35	300.67	319.80	963.13	1344.77
Improvement	↑ 10.65%	↑ 8.50%	↑ 8.90%	↑ 13.18%	↑ 10.83%	↑ 26.69%	↑ 17.65%

Table B.5. DataLight performance under different action durations when trained with mixed COD (ATT in seconds)

Action duration	JN			HZ		NY	
	JN1	JN2	JN3	HZ1	HZ2	NY1	NY2
10s	264.74	229.83	233.15	266.25	305.47	978.94	1258.38
15s	250.19	232.40	228.76	271.46	299.79	959.41	1268.76
20s	253.12	243.04	237.47	281.09	303.46	969.19	1282.31
25s	263.65	255.19	248.73	292.70	310.98	922.30	1259.75